

Resuspension of particle-bound heavy metals from soil and seawater

Wind re-suspension of particle-bound heavy metals (like lead and cadmium) from soil and seawater appears to be important process affecting ambient concentration and deposition of these pollutants, particularly, in areas with low direct anthropogenic emissions.

In mineral dust production models the process of wind erosion and suspension of dust aerosol from the ground is commonly parameterized as combination of two major processes: saltation and sandblasting [e.g. *Gomes et al., 2003; Zender et al., 2003; Gong et al., 2003*]. The first process (saltation) presents horizontal movement of large soil aggregates driven by wind stress. These aggregates are too heavy to be directly suspended by wind in usual conditions. Instead, they are moved by wind stress close to the surface jumping from one place to another. When the saltating aggregates impact the ground they can eject much smaller particles (few micrometers), which can be easily suspended by wind and transported far away from the source region. This process is called the sandblasting.

Saltation

The saltation process is characterized by the critical wind stress value, over which movement of soil particles can be initiated. This critical wind stress can be described by the threshold wind friction velocity, which depends on the soil particle size, soil wetness, and protection of the erodible soil by roughness elements (drag partitioning). In order to characterize this threshold friction velocity (U_t^*) in the model we used a simplified empirically based parameterization proposed by *Marticorena and Bergametti [1995]*:

$$\begin{cases} U_t^* = \frac{0.129k}{(1.928Re^{0.092} - 1)^{0.5}}, & Re \leq 10 \\ U_t^* = 0.129k(1 - 0.858 \exp(-0.0617(Re - 10))), & Re > 10, \end{cases} \quad (1)$$

where

$$k = \sqrt{\frac{D_s}{\rho_a} \left(\rho_s g + \frac{6 \cdot 10^{-7}}{D_s^{5/2}} \right)}, \quad Re = 1.755D_s^{1.56} + 0.38.$$

Here D_s is the soil particle size, ρ_a and ρ_s are air and soil mass densities, respectively; g is the gravity acceleration.

The threshold value increases for very small and very large particles and has a minimum corresponding approximately to 75 μm (Fig. 1).

The saltation threshold is affected by soil moisture content. Soil water retention (because of interparticle capillary and molecular adsorption forces) leads to cohesion of soil particles and increase of the wind erosion threshold. In the first version of the re-suspension scheme we used a simplified approach to account for the soil moisture effect suggested by *Grini et al.* [2005]. It is based on rainfall events and implements the following assumptions:

- The dust production is stopped if precipitation during the last 24 hours exceeds 0.5 mm.
- The period without the dust production (in days) is equal to precipitation amount (in mm) during the last 24 hours.
- The dust production is resumed if no rain has fallen in the last 5 days.

Under natural conditions wind stress is commonly sharing between erodible and non-erodible surfaces. It leads to decrease of actual friction velocity describing wind momentum transfer to the erodible surface and initiation of the saltation process. Extend of the wind drag partition depends both on size and density of non-erodible roughness elements. In the current dust suspension scheme we apply parameterization based on the drag partition scheme developed by *Shao and Yang* [2005]. According to this scheme the total drag is partitioned into a pressure drag on the roughness elements τ_p , skin drag on the surface of the roughness elements τ_b , and skin drag on the underlying surface τ_s :

$$\tau = \tau_p + \tau_b + \tau_s \quad (2)$$

Only the drag on the underlying surface is responsible for wind erosion and dust suspension. Following *Shao and Yang* [2005] relative contribution of the surface drag can be presented as:

$$\frac{\tau_s}{\tau} = \left(1 - \frac{\beta\lambda_{ef}}{1 + \beta\lambda_{ef}} \right) \exp(-5\eta), \quad (3)$$

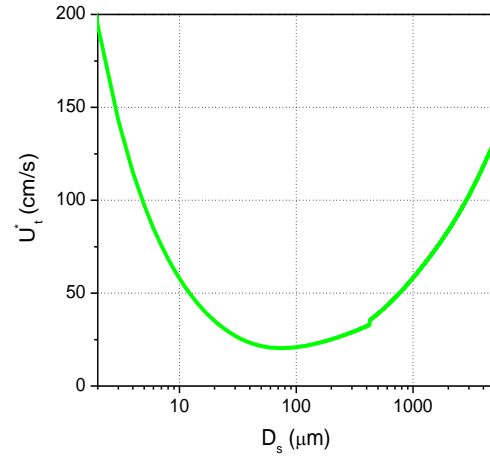


Fig. 1. Threshold friction velocity as a function of soil particles size

where $\beta = C_R/C_S$ is the ratio of the drag coefficient for isolated roughness elements to that for bare surface; λ_{ef} is effective frontal area index representing the effect of mutual sheltering of roughness elements defined as:

$$\lambda_{ef} = \frac{\lambda}{(1 - \eta)^{0.1}} \exp\left(-\frac{6\lambda}{(1 - \eta)^{0.1}}\right) \quad (4)$$

λ and η are the frontal area index and skin area index characterizing density and form of roughness elements, respectively.

The frontal area index is generally defined as $\lambda = nbh$; where b and h are the characteristic width and height of roughness elements, and n is the number of roughness elements per unit surface area. The value $\sigma = \eta/\lambda$ (called as the aspect ratio of roughness elements) characterizes average ratio of basal area to profile area of the roughness elements. *Marticorena et al.* [2006] measured dimensions of different obstacles in arid and semi-arid areas and obtained average aspect ratios close to 2. Thus, we set $\eta = 2\lambda$ in the dust suspension scheme.

Wind friction velocity is defined as $U^* = \sqrt{\tau/p_a}$, therefore ratio of friction velocity $(U^*)_s$ corresponding to erodible surface to the whole friction velocity can be calculated as follows:

$$\frac{(U^*)_s}{U^*} = \sqrt{\frac{\tau_s}{\tau}} = \sqrt{1 - \frac{\beta\lambda_{ef}}{1 + \beta\lambda_{ef}} \exp(-5\lambda)}. \quad (5)$$

The fraction of smooth friction velocity quickly decreases while roughness density increases (Fig. 2). Values of the drag coefficients ratio typically vary from 100 to 200 for different types of rough surfaces [*Shao and Yang, 2005*]. As seen from the figure the fraction of smooth friction velocity only slightly depends on this parameter. Therefore a fixed value $\beta = 150$ is accepted in the scheme. The frontal area index significantly varies for different rough surfaces and land cover types. According to field measurements and conditions of wind tunnel experiments [*Marticorena et al., 2006; Shao and Yang, 2005*] this parameter commonly ranges from 0.001 to 0.2. In tentative calculations we accepted the following values of the frontal area index: 0.01 for bare land and urban areas, 0.002 for arable land during cultivation period. However, more extensive

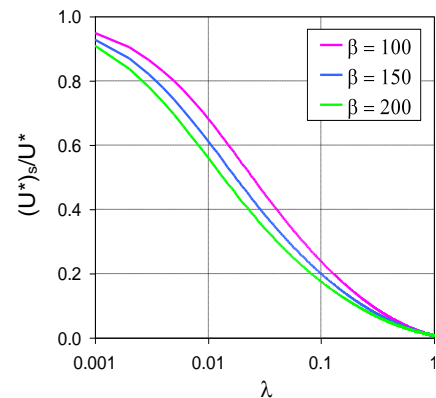


Fig. 2. Fraction of wind friction velocity related to erodible surface as a function of

analysis is required for attribution the frontal area index to different land cover categories and different locations.

Another process affecting wind erosion and saltation of soil particles is the Owen effect [Owen, 1964] responsible for positive feedback of saltation on wind friction velocity. Saltating soil aggregates interact with underlying surface and transfer part of wind momentum to the ground. It leads to increase of the wind shear stress, which can be expressed in increase of the wind friction velocity. Gillette *et al.* [1998] derived a simple formula for this effect using field measurements at dry Owens Lake:

$$\Delta U^* = 0.003(U_{10} - U_{10,t})^2 \quad (6)$$

where ΔU^* (in m/s) is increase of wind friction velocity due to the Owen effect; U_{10} and $U_{10,t}$ (in m/s) are the wind speed and the threshold wind speed at 10 m height, respectively.

Once the wind friction velocity exceeds the threshold value, the vertically integrated size-resolved saltation flux is given in the following form [Gomes *et al.*, 2003]:

$$F_h(D_s) = \frac{K\rho_a}{g} (U^* - U_t^*)(U^* + U_t^*)^2 \quad (7)$$

The constant K in this expression reflects possibility of the limitation of soil aggregates supply because of depletion of loose material on the surface. According to Gomes *et al.* [2003] this constant is close to unity for sandy soils but much lower (about 0.02) for soils with elevated clay content where wind erosion is inhibited by crust formation after rainfalls. Thus, we adopted $K = 1$ for deserts, $K = 0.02$ for other bare soils and urban areas and $K = 0.1$ for all cultivated agricultural soils.

An example of the saltation flux dependence on the soil particle size is presented in Fig. 3a. As seen from the figure the wind of a given stress is able to involve into the movement soil aggregates with the particle size from the certain interval (35-200 μm). The integrated saltation flux as a function of the wind friction velocity is illustrated in Fig. 3b.

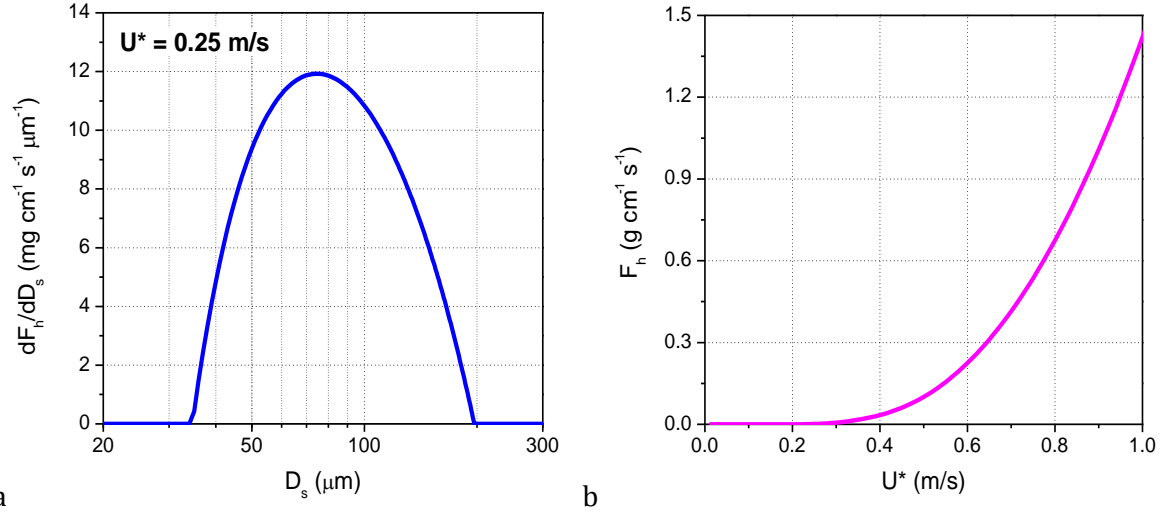


Fig. 3. Density of the saltation flux as a function of soil particles size (a) and dependence of the integrated saltation flux on wind friction velocity (b)

Soil properties data

In general the integral saltation flux strongly depends on size distribution of soil aggregates. Indeed, in natural soils small particles (below 20 μm) never occur in free state, but are embedded in larger soil aggregates (up to a few centimetres) by cohesion forces. *Chatenet et al.* [1996] used the dry sieving technique to derive four typical populations of arid soils. It was suggested that size distribution of any soil could be presented as a combination of these populations according to its mineralogical type. Thus, a continuous multi-modal distribution of soil aggregates can be presented by a combination of lognormal functions:

$$\frac{dM}{dD_s} = \frac{1}{D_s \sqrt{2\pi}} \sum_j \frac{\varepsilon_j}{\ln \sigma_j} \exp\left(\frac{(\ln D_s - \ln \overline{D_{s,j}})^2}{-2 \ln^2 \sigma_j}\right), \quad (8)$$

where $\overline{D_{s,j}}$ is mass median diameter (MMD) of the j^{th} mode; σ_j is its geometric standard deviation; and ε_j is mass fraction of particles of the j^{th} mode.

Definition of soil texture is based on Harmonized World Soil Dataset (HWSD) [FAO, 2009]. These data present spatial distribution of sand, silt and clay content with resolution 30x30 arc seconds (about 1x1 km^2). These data are used to calculate grid-cell averaged content of sand, silt and clay and to define types of soil texture in each land gridcell of the EMEP mesh.

Each soil type was associated with certain size distribution of soil aggregates based on the dry sieving technique measurements by *Chatenet et al.* [1996]. We used definitions

of soil size distribution derived for major arid soil types by *Marticorena and Bergametti* [1997]. According to this work size distribution of soil aggregates can be presented as a combination of three soil populations with definite lognormal distribution function. Parameters of the soil populations for eight soil texture types appearing in Europe are presented in Table 1.

Table 1. Parameters of soil size distribution for different soil texture types

Soil texture type	Soil population 1			Soil population 2			Soil population 3		
	MMD	σ	%	MMD	σ	%	MMD	σ	%
Sand	690	1.6	100	-	-	-	-	-	-
Loamy sand	690	1.6	90	210	1.8	10	-	-	-
Sandy loam	690	1.6	80	210	1.8	20	-	-	-
Loam	690	1.6	31.25	210	1.8	31.25	125	1.6	37.5
Silt loam	520	1.6	75	-	-	-	125	1.6	25
Silt	520	1.6	50	-	-	-	125	1.6	50
Sandy clay loam	-	-	-	210	1.8	100	-	-	-
Clay loam	-	-	-	210	1.8	62.5	125	1.6	37.5

Sandblasting

The sandblasting model for dust suspension has been developed by *Alfaro et al.* [1997; 1998]. Based on the wind tunnel experiments they derived that the dust particles released by sandblasting from the saltating aggregates of different natural soils can be sorted into three lognormal modes (do not mix up with soil populations). Characteristics of the dust modes are presented in Table 2.

Table 2. Characteristics of size distribution modes for dust particles released by sandblasting [Alfaro and Gomes, 2001]

Mode	$e_i, kg\ m^2/s^2$	$d_i, \mu m$	σ_i
1	$3.61 \cdot 10^{-7}$	1.5	1.7
2	$3.52 \cdot 10^{-7}$	6.7	1.6
3	$3.46 \cdot 10^{-7}$	14.2	1.5

According to the sandblasting model the vertical dust flux corresponding to i^{th} can be presented in the following form [Alfaro and Gomes, 2001]:

$$F_{v,i} = \int_{D_s} F_h(D_s) \alpha_i(D_s) \frac{dM}{dD_s} dD_s, \quad i = \overline{1,3}, \quad (9)$$

where the efficiency of the sandblasting process is given by:

$$\alpha_i(D_s) = \frac{\pi}{6} \rho_s \beta \frac{p_i d_i^3}{e_i} \quad (10)$$

Here $\beta = 163 \text{ m/s}^2$ is an empirical constant; p_i is the fraction of kinetic energy of a soil aggregate required to release dust particles of mode i , d_i is the aerosol mass median diameter of mode i ; and e_i is binding energy of aerosol particles for mode i .

The fraction p_i of the aerosol modes release depends on the kinetic energy of an individual soil aggregate:

$$e_c = \frac{100}{3} \pi \rho_s D_s^3 U^{*2} \quad (11)$$

A scheme of the dependence is presented in Table 3. The binding energies e_i correspond to values presented in Table 2. As seen from the table the higher kinetic energy of a soil aggregate e_c the more probability to eject finer particles (Mode 1).

Table 3. Fractions (p_i) of the dust aerosol modes release as a function of the kinetic energy e_c of an individual soil aggregate

	$e_c < e_3$	$e_3 < e_c < e_2$	$e_2 < e_c < e_1$	$e_1 < e_c$
Mode 1 (p_1)	0	0	0	$(e_c - e_1)/(e_c - e_3)$
Mode 2 (p_2)	0	0	$(e_c - e_2)/(e_c - e_3)$	$(1 - p_1)(e_c - e_2)/(e_c - e_3)$
Mode 3 (p_3)	0	1	$1 - p_2$	$1 - p_1 - p_2$

An example of calculated relative fractions of the dust aerosol modes as a function of soil aggregates size are shown in Fig. 4a for given wind friction velocity. As seen from the figure sandblasting of larger soil aggregates, which have higher kinetic energy, releases smaller dust particles. Figure 4b presents an example of size distribution of the vertical dust flux for given wind friction velocity and size distribution of saltating soil aggregates. As seen the Mode 1 corresponds mostly to fine particles (below $2 \mu\text{m}$), where as two other modes present coarse particles ($5\text{-}20 \mu\text{m}$).

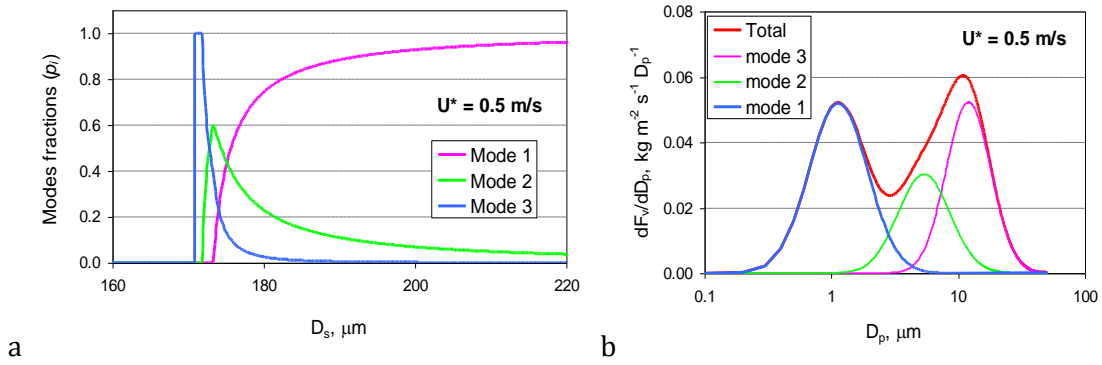


Fig. 4. Fractions of dust aerosol modes as functions of soil aggregates size (a) and size distribution of vertical dust flux (b)

Figure 5 presents examples of size distribution of the vertical dust flux from different soil types. Dependence of dust suspension flux on wind friction velocity for different soil types is illustrated in Fig. 6 along with contribution of three aerosol modes to the total flux.

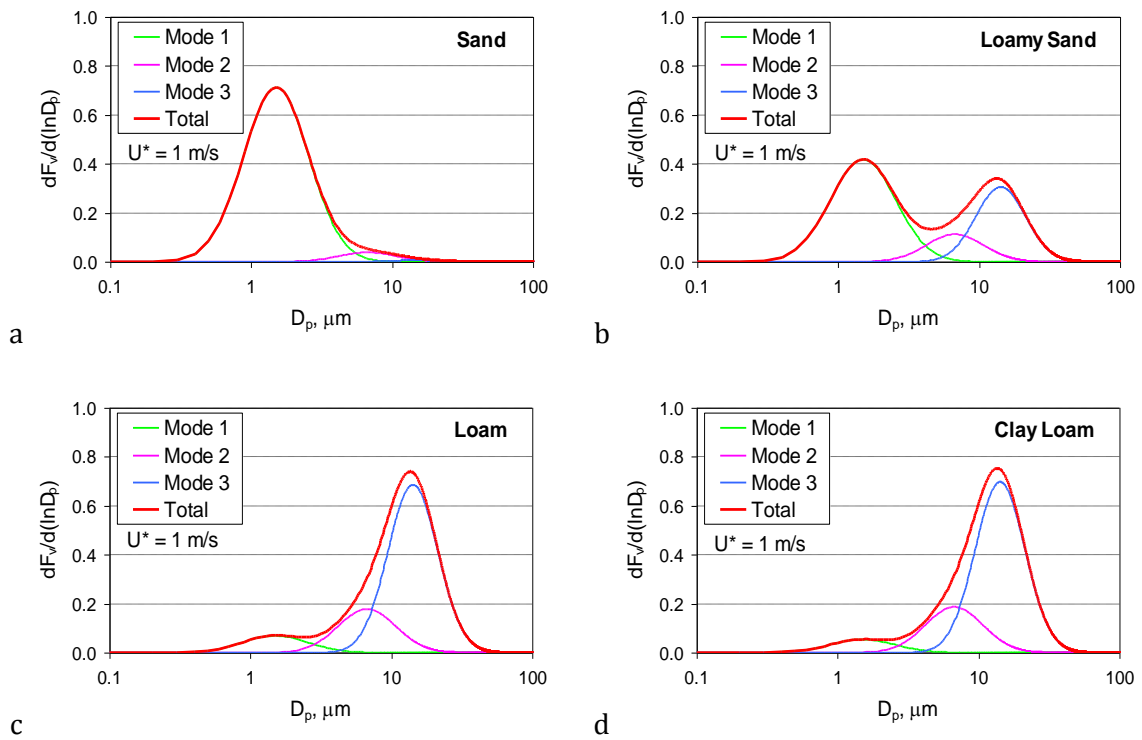


Fig. 5. Size distribution of vertical dust flux for different soil types: (a) – sand; (b) – loamy sand; (c) – loam; (d) – clay loam

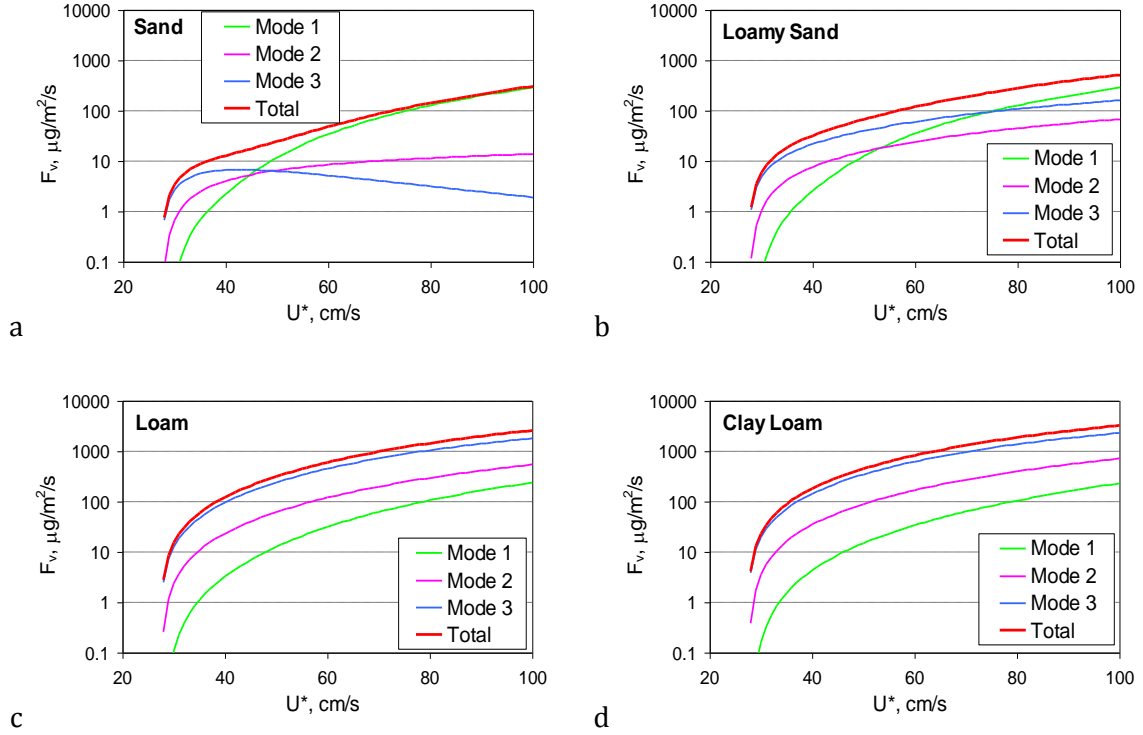


Fig. 6. Vertical dust flux as a function of the wind friction velocity for different soil types: (a) – sand; (b) – loamy sand; (c) – loam; (d) – clay loam

Sea-salt aerosol suspension

Description of sea-salt generation and wind suspension from the sea surface has also been included into the model. For this purpose we applied the empirical Gong-Monahan parameterization of the vertical number flux density [Gong, 2003]:

$$\frac{dF_n}{dR_p} = 1.373 U_{10}^{3.41} R_p^{-A} (1 + 0.057 R_p^{3.45}) 10^{1.6 \exp(-B^2)}, \quad (12)$$

where

$$A = 4.7(1 + \Theta R_p)^{-0.017 R_p^{-1.44}}, \quad B = 1 - \frac{\log R_p}{0.433}.$$

Here R_p is the sea-salt aerosol radius; U_{10} is wind speed at 10 m height; and $\Theta = 30$ is an adjustable parameter that controls the shape of the sub-micron size distribution.

The size distribution of the vertical sea-salt aerosol mass flux based on this parameterization is shown in Fig. 7a for different wind speeds. Figure 7b illustrates dependence of the integral sea-salt aerosol flux on wind speed at 10 m height for different cut-off aerosol diameters. In the following calculations we used the cut-off

value of aerosol diameter equal to 10 μm , since larger particles can hardly be transported far from the ocean coastal areas.

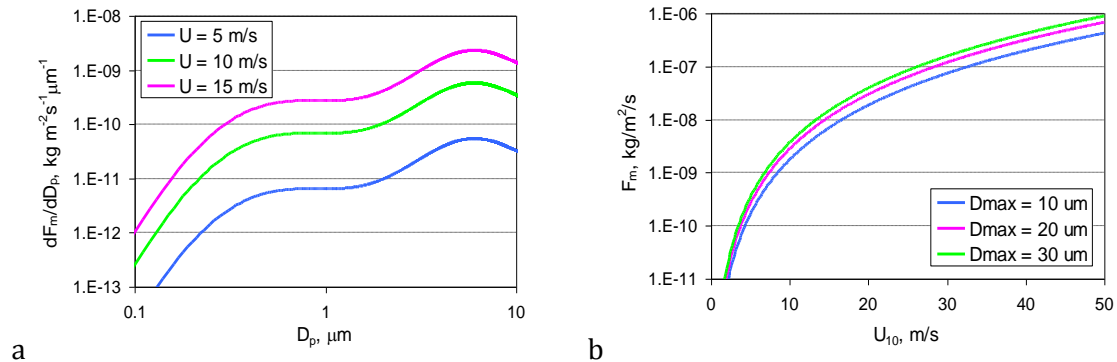


Fig. 7. Sea-salt aerosol mass flux as a function of particle size (a) and dependence of the sea-salt flux on wind speed at 10 m height for different cut-off aerosol diameters (b)

Re-suspension of heavy metals from soil and seawater

To estimate heavy metal emission with dust suspension from soil it is necessary to know content of these metals in erodible soils. For this purpose detailed measurement data on heavy metals concentration in topsoil from the Geochemical Atlas of Europe developed under the auspices of the Forum of European Geological Surveys (FOREGS) [*Salminen et al.*, 2005; www.gtk.fi/publ/foregsatlas/] were used. The data cover most parts of Europe (excluding Eastern European countries) with more than 2000 measurement sites.

The kriging interpolation was applied to obtain spatial distribution of heavy metal concentration in soil. For Eastern Europe as well as for the rest of the model domain (Africa, Asia) we used default concentration values 0.2 mg/kg and 15 mg/kg for cadmium and lead, respectively, based on the literature data [*Nriagu*, 1980; *Reimann and Cariat*, 1998].

It should be noted that these data mostly reflect background concentrations in residual and sedentary soils. Particularly, soil sampling was avoided from urban areas and areas with agricultural activities. Besides, the organic layer was removed from undisturbed soil samples [*Salminen et al.*, 2005]. On the other hand, Pb and Cd concentrations measured in humus are several times higher than those in underlying soil. Similar enrichment of the upper soil layer with heavy metals by an order of magnitude was obtained by *Alriksson* [2001] for forest soils and by *Linde et al.* [2001] for urban soils. Thus, one can expect significant enrichment of the upper skin layer of soil available for wind erosion in comparison with topsoil concentrations. Moreover, measured concentrations of heavy metal concentrations road dust in urban areas are typically much higher than concentrations in soils [e.g., *Charlesworth et al.*, 2011, *Christoforidis*

and Stamatis, 2009, Ordóñez et al., 2015]. Agricultural soil can be additionally enriched with cadmium due to its input with fertilisers and sewage sludge. Therefore enrichment factors for the upper layer of different soil types are used in modelling of wind re-suspension. It is assumed that the enrichment factor is proportional to the accumulated deposition. Coefficients of proportionality were selected to reach reasonable fit between modelled and observed concentrations and wet deposition.

In order to estimate heavy metal re-suspension with sea-salt aerosol we used the emission factors: 4 mg/kg for lead and 40 µg/kg for cadmium, derived from the literature [Nriagu, 1980, Richardson et al., 2001].

-
- Alfaro S.C. and L. Gomes [2001] Modeling mineral aerosol production by wind erosion: Emission intensities and aerosol size distributions in source areas. *Journal of Geophysical Research*, vol. **106**, No. D16, pp.18,075 – 18,084.
- Alfaro S.C., Gaudichet A., Gomes L. and M. Maillé [1998] Mineral aerosol production by wind erosion: aerosol particle sizes and binding energies. *Geophysical Research Letters*, vol. **25**. No. 7, pp.991– 994.
- Alfaro S.C., Gaudichet A., Gomes L., Maillé M. [1997] Modeling the size distribution of a soil aerosol produced by sandblasting. *Journal of Geophysical Research*, vol.**102**, pp.11239–11249.
- Alriksson A. [2001] Regional variability of Cd, Hg, Pb and C concentrations in different horizons of Swedish forest soils. *Water, Air, and Soil Pollution: Focus*, vol. **1**, No. 3-4, pp.325-341.
- Charlesworth, S., De Miguel, E. and Ordóñez, A. [2011]. A review of the distribution of particulate trace elements in urban terrestrial environments and its application to considerations of risk. *Environ Geochem Health* (2011) **33**: 103. <https://doi.org/10.1007/s10653-010-9325-7>.
- Chatenet B.B., Marticorena B.B., Gomes L. and G. Bergametti [1996] Assessing the size distribution of desert soils erodible by wind. *Sedimentology*, vol. **43**, pp. 901 – 911.
- Christoforidis A. and Stamatis N. [2009]. Heavy metal contamination in street dust and roadside soil along the major national road in Kavala's region, Greece. *Geoderma* **151** (2009) 257–263.
- FAO/IIASA/ISRIC/ISS-CAS/JRC [2009] Harmonized World Soil Database (version 1.1). FAO, Rome, Italy and IIASA, Laxenburg, Austria.
- Gillette D. A., Marticorena B., Bergametti G. [1998] Change in the aerodynamic roughness height by salting grains: Experimental assessment, test of theory, and operational parameterization. *Journal of Geophysical Research*, vol. **103**, No. D6, pp. 6203-62-09.
- Gomes L., Rajot J.L., Alfaro S.C. and A. Gaudichet [2003] Validation of a dust production model from measurements performed in semi-arid agricultural areas of Spain and Niger. *Catena*, vol. **52**, pp. 257 – 271.
- Gong S.L. [2003] A parameterization of sea-salt aerosol source function for sub- and super-micron particles. *Global Biogeochemical Cycles*, vol. **17**, No. 4, p. 1097.
- Gong S.L., Zhang X.Y., Zhao T.L., McKendry I.G., Jaffe D.A., Lu N.M. [2003] Characterization of soil dust aerosol in China and its transport and distribution during 2001 ACE-Asia: 2. Model simulation and validation. *Journal of Geophysical Research*, **108**(D9), 4262
- Grini A., Myhre G., Zender C.S. and I.S.A. Isaksen [2005] Model simulations of dust sources and transport in the global atmosphere: Effects of soil erodibility and wind speed variability. *Journal of Geophysical Research*, vol. **110**, pp.D02205.
- Linde M., Bengtsson H., Öborn I. [2001] Concentrations and pools of heavy metals in urban soils in Stockholm , Sweden. *Water, Air, and Soil Pollution: Focus*, vol. **1**, No. 3-4, 83-101.
- Marticorena B. and G. Bergametti [1995] Modeling the atmospheric dust cycle: 1. Design of a soil-derived dust emission scheme. *Journal of Geophysical Research*, vol. **100**, No. D8, pp. 16,415 – 16,430.
- Marticorena B., Bergametti G, and B. Aumont [1997] Modeling the atmospheric dust cycle: 2. Simulation of Saharan dust sources. *Journal of Geophysical Research*, vol. **102**, No. D4, pp. 4387 – 4404.

- Marticorena B., Kardous M., Bergametti G., Callot Y., Chazette P., Khatteli H., Le Hégarat-Masclé S., Maillé M., Rajot J.-L., Vidal-Madjar D., Zribi M. [2006] Surface and aerodynamic roughness in arid and semiarid areas and their relation to radar backscatter coefficient. *Journal of Geophysical Research*, vol. **111**, F03017.
- Nriagu J.O. [1980] Cadmium in the atmosphere and in precipitation. In: J.O. Nriagu (ed.), *Cadmium in the environment, Part I: Ecological cycling*, John Wiley & Sons, New York, pp. 71-114.
- Ordóñez A, Álvarez R., De Miguel E., and Charlesworth S. [2015]. Spatial and temporal variations of trace element distribution in soils and street dust of an industrial town in NW Spain: 15 years of study. *Science of the Total Environment* 524–525 (2015) 93–103.
- Owen P.R. [1964] Saltation of uniform sand grains in air. *Journal of Fluid Mechanics*, vol. **20**, pp.225-242.
- Richardson G.M., Garret R., Mitchell I., Mah-Paulson M. and T.Hackbarth [2001] Critical Review of natural global and regional emissions of six trace metals to the atmosphere. Final Report. Risklogic Scientific Services, Inc, 52p.+tables.
- Riemann C. and P. de Caritat [1998] *Chemical elements in the Environment, Factsheets for the Geochemist and Environmental Scientist*. Springer, New York, 398 pp.
- Salminen R. (Chief-editor), Batista M. J., Bidovec M., Demetriades A., De Vivo B., De Vos W., Duris M., Gilucis A., Gregorauskiene V., Halamic J., Heitzmann P., Lima A., Jordan G., Klaver G., Klein P., Lis J., Locutura J., Marsina K., Mazreku A., O'Connor P. J., Olsson S.Å., Ottesen R.-T., Petersell V., Plant J.A., Reeder S., Salpeteur I., Sandström H., Siewers U., Steenfelt A., Tarvainen T. [2005] *Geochemical Atlas of Europe. Part 1: Background Information, Methodology and Maps*. Espoo, Geological Survey of Finland, 526 pages, 36 figures, 362 maps.
- Shao Y. and Yang Y. [2005] A scheme for drag partition over rough surfaces. *Atmospheric Environment*, vol. **39**, pp.7351-7361.
- Zender C. S., Bian H. and D. Newman [2003] Mineral dust entrainment and deposition (DEAD) model: description and 1990s dust climatology. *Journal of Geophysical Research*, vol. **108**, No. D14, p. 4416.